Improved Turbo SENSE with Iterated Conjugate Gradient Phase Refinement

C. Lew[1], D. Spielman[1], F. Chan[1], R. Bammer[1]

[1]Stanford University, Stanford, CA, United States

Introduction: Phase-constrained parallel imaging, notably phase-constrained GEM(1) and turboSENSE(2,3), has been shown to have better SNR characteristics compared to SENSE (4) at the same reduction factor. These techniques double the number of SENSE equations by separating the real and imaginary components and consequently narrows the solution vector for the minimal least-squares solution. In effect, the g-factor is lowered. Having an accurate phase estimate is key to obtaining a good reconstruction. Often, the phase is derived from the calibration measurements. Problems arise when the phase requires high resolution to capture sharp phase profiles such as air-tissue or water-fat interfaces. The residual phase errors can leave aliasing artifacts in the turboSENSE reconstruction. Since the phase is incorporated into the real and imaginary equations in the turboSENSE matrix, phase errors directly translate into errors in the magnitude reconstruction. Field map inhomogeneity issues in least squares estimation of multi-point Dixon imaging are similar to the phase errors with turboSENSE. Reeder, et al (5), have demonstrated an iterative method for least squares estimation of field map inhomogeneity in multi-point Dixon imaging. Here, we present a similar method to improve the phase estimate.

0) Let **C** be the initial coil calibration that is separated into real and imaginary parts. Let **S** be the acquired data separated into real and imaginary parts.
1) Perform turboSENSE recon for the turboSENSE equation $\mathbf{S} = \mathbf{C}\rho$
2) Determine the residual error $\mathbf{\Delta S}=\mathbf{S}-\mathbf{C}\rho_{\mathbf{recon}}$
3) If error norm converges, stop
4) Compute residual error system of

equations $\Delta\mathbf{S} \approx \sum_n \left.\frac{\partial(\mathbf{C}\rho)}{\partial\theta_n}\right|_{\rho_{recon}} \Delta\theta_n + \sum_n \left.\frac{\partial(\mathbf{C}\rho)}{\partial\rho_n}\right|_{\rho_{recon}} \Delta\rho_n$

5) Solve for $\Delta\theta_1, \Delta\theta_2, \ldots \Delta\theta_n, \Delta\rho_1, \Delta\rho_2, \ldots \Delta\rho_n$

6) Update the phase with $\Delta\theta_1, \Delta\theta_2, \ldots \Delta\theta_n$ to create a new **C**
7) Go back to 1)

Figure 1

Theory: The proposed method employs an iterative conjugate gradient method similar to Reeder's method to update the phase estimate for turboSENSE reconstruction. Initially, a turboSENSE reconstruction is performed with the coil calibrations obtained from a separate scan or internal self-calibration. The initial phase estimate has already been absorbed into the calibration measurement. For a reduction factor of *n* (R=*n*), turboSENSE reconstruction is performed on each set of *n* aliased pixels for the entire image. Next, the residual error is computed. The error is approximated to be the total derivative of the SENSE equations with respect to the set of aliased magnitude and phase pixels. The derivative is separated into phase and magnitude changes. Omitting higher order terms, this error represents a new set of equations that can be solved via least squares. The phase error for the *n* pixels is solved and used to update the phase in the original turboSENSE reconstruction matrix. A new turboSENSE reconstruction is performed. This process repeats until convergence of the residual error to a minimum. Figure 1 shows a summary of the algorithm.

Methods: The coil calibrations were acquired with an *in-vivo* phase-contrast gradient echo sequence from a GE Signa 1.5T scanner with a 256x160 imaging matrix in Cartesian k-space with 6 views per segment. The calibrations were performed on a separate scan with a 4-channel torso coil. The sensitivity matrix was calculated by dividing the individual coil calibrations by the sum-of-squares image. The undersampled acquisition was also performed with the same sequence. Reduction factors of 2, 3, and 4 were used. Iterations were performed until there was a less than 1% change in the residual norm from the previous iteration.

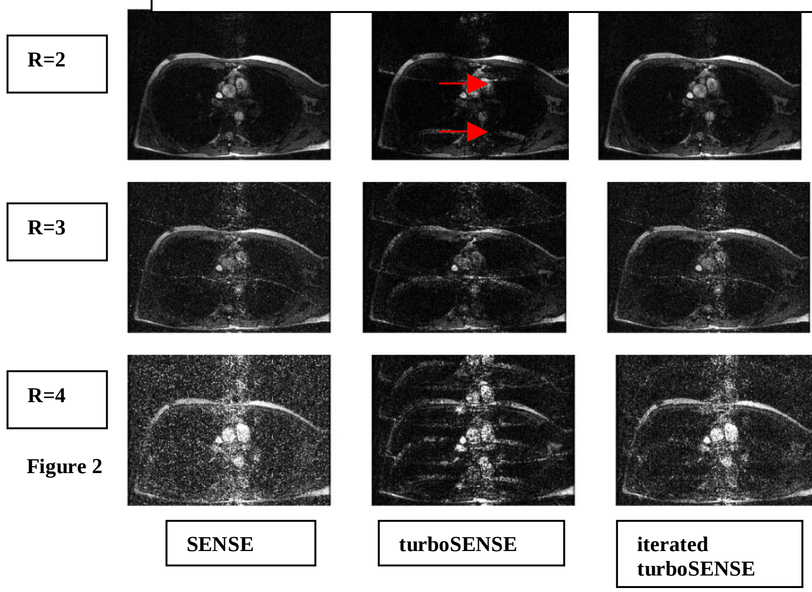

Figure 2

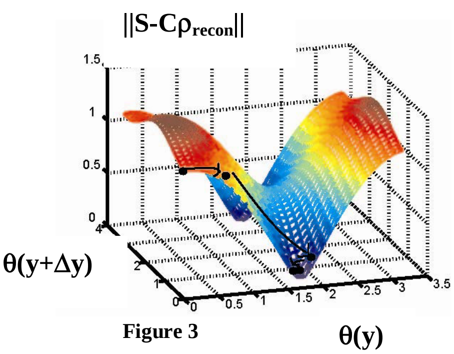

Figure 3

Results: Figure 2 shows the magnitude images for reduction factors of 2, 3, and 4 for SENSE, the initial turboSENSE reconstruction, and the final iterated turboSENSE reconstruction. Specifically for R=2, figure 3 shows a mesh plot of the residual error norm as a function of phase perturbations for pixel (140,90) and its aliased counterpart at (140,186). Since the error is periodic over π, only the range from 0 to π is shown. The trajectory of the (140,90) pixel during iterated turboSENSE is shown as well. Refer to the red arrows on figure 2 for the pixel location.

Discussion: It is clearly shown that the iterated turboSENSE improves upon the initial turboSENSE reconstruction. Iterated turboSENSE removed many of the aliasing chest wall artifacts and cleaned up areas in the aorta and pulmonary artery. Compared to SENSE, iterated turboSENSE is visually at least as good for R=2 and R=3. In R=4, it has a clear performance gain over SENSE in terms of residual aliasing and noise enhancement. The chest wall in iterated turboSENSE is more clearly delineated than those of SENSE and turboSENSE. The lower g-factors in turboSENSE clearly manifest for this case. The lack of difference for R=2 and R=3 may be attributed to the overdetermination in SENSE and turboSENSE, which is sufficient to produce a reconstruction not limited by the g-factor. Future work would be to improve the iterative approach to exploit the lower g-factor of turboSENSE further. Also, this iterative technique may be used for SENSE as well.

References: 1. Willig-Onwuachi, J.D., et al. Proceedings for the ISMRM 11th annual, 19, 2003. 2. Bammer, R., PhD Thesis, Graz University of Technology, Graz, Austria, 2000. 3. Lew, C., et al, 2646, ISMRM 2003. 4. Pruessman, K.P., et al. MRM, 42:952-962, 1999. 5. Reeder, S., et al. MRM, 51:35-45, 2004.

Acknowledgments: Support was provided by GE Medical Systems, NIH grants RR09784, 1R01EB002771, 1R01NS35959, and GM08412, Center of Advanced MR Technology at Stanford P41RR09784, the Oak Foundation, and the Lucas Foundation.